Resolved Sideband Raman Cooling of an Optical Phonon in Semiconductor Materials

Jun Zhang[1,2,*], *Qing Zhang*[1], *Xingzhi Wang*[1], *Leong Chuan Kwek*[3,4], *and Qihua Xiong*[1,5,6,*]

[1]Division of Physics and Applied Physics, School of Physical and Mathematical Sciences, Nanyang Technological University, 637371, Singapore.

[2]State Key Laboratory of Superlattices and Microstructures, Institute of Semiconductors, Chinese Academy of Sciences, Beijing, 100083, China

[3]Centre for Quantum Technologies, National University of Singapore, 3 Science Drive 2, 117543, Singapore

[4]National Institute of Education and Institute of Advanced Studies, Nanyang Technological University, 1 Nanyang Walk, 637616, Singapore

[5]NOVITAS, Nanoelectronics Center of Excellence, School of Electrical and Electronic Engineering, Nanyang Technological University, 639798, Singapore.

[6]MajuLab, CNRS-UNS-NUS-NTU International Joint Research Unit, UMI 3654, Singapore

*Correspondence should be addressed to Email: zhangjwill@semi.ac.cn, Qihua@ntu.edu.sg

The radiation pressure of light has been widely used to cool trapped atoms or the mechanical vibrational modes of optomechanical systems. Recently, by using electrostrictive forces of light, spontaneous Brillouin cooling and stimulated Brillouin excitation of whispering-gallery type acoustic modes have been demonstrated. The laser cooling of specific lattice vibrations in solids (*i.e.*, phonons) proposed by Dykman in 1980s, however, still remains sparsely investigated. Here we demonstrate the first strong spontaneous Raman cooling and heating of longitudinal optical phonon (LOP) with a 6.23 THz frequency in polar semiconductor zinc telluride nanobelts. We use the exciton to resonate and assist photo-elastic Raman scattering from LOPs due to strong exciton-LOP coupling. By detuning the laser pump to lower (higher) energy resolved-sideband to make spontaneous scattering photon resonate with exciton at anti-Stokes (Stokes) frequency, the dipole oscillation of the LOPs is beat and photo-elastically attenuated (enhanced) to a colder (hotter) state.

Spontaneous Raman and Brillouin scattering is described in terms of the statistical nature of the fluctuations in the optical properties of the medium[1,2]. Incident photons are inelastically scattered to lower (Stokes) or higher (anti-Stokes) frequency via electron-phonon interactions, corresponding to the creation or annihilation of phonons respectively. When the scattered photon frequency resonates with an internal state (such as electronic transition), *i.e.* $\omega_{internal} = \omega_{laser} \pm n\Omega_{phonon}$ (n is an integer), and the corresponding frequency of phonon is larger than the damping of internal state, *i.e.* $\Omega_{phonon} > \gamma_{internal}$, the corresponding scattering peak of $\pm n\Omega_{phonon}$ exhibits the highest intensity. Depending on the resonant situation, the energy flow direction of scattering can be controlled either as phonon heating pumped at blue-resolved-sideband (Stokes resonance) or phonon cooling at red-resolved-sideband pumping (anti-Stokes resonance). The highest cooling or heating efficiency is achievable at the first resolved-sideband, *i.e.* n=1. Such technique is called the resolved-sideband cooling, which has been demonstrated at low frequency oscillators in the trapped atoms[3-7] and cavity optomechanical systems[8-11]. Resolved-sideband cooling plays an important role in cold atom study, quantum ground state preparation and coherent quantum-state manipulation[4,5,7,12-14].

In solids, laser cooling research mainly focuses on the anti-Stokes photoluminescence cooling, in which the temperature of the whole solid thus the entire distribution of internal vibrational modes of solids is cooled down[15-17]. As an extended work of resolved-sideband cooling in atoms, laser cooling of one specific phonon mode in solid is important in the study of solid-based quantum technique. In theory, Dykman discussed the possibility of cooling, heating and amplification of specific phonon in solids by similar physics of resolved-sideband cooling in atoms[18,19]. In experiment, resolved-sideband cooling of whispering-gallery type acoustic modes in Brillouin scattering regime has been demonstrated[20]. These works have raised the question of whether it is possible to cool optical phonon modes in solid by means of a Raman process. In order to achieve Raman anti-Stokes cooling, the energetically favorable Stokes process leading to heating must be suppressed[20]. However, as the high frequency optical phonons have higher dissipation rate than acoustic phonons, eliminating the Stokes process is not readily practical in solid state materials[20,21]. Herein, we demonstrate the reverse of the energy flow direction in spontaneous Raman scattering in zinc telluride (ZnTe) nanobelts by detuning the pump laser relative to the exciton resonance with an energy of the LOP. Being different from the Brillouin cooling of acoustic modes which is dominated by electrostrictive forces, the “radiation forces” in Raman cooling of LOP is due to photoelastically induced Fröhlich forces[2] (Supporting Information), where long-wavelength longitudinal optical (LO) phonon can lead to the separation of the oppositely charged atoms and thus generate a macroscopic electric field inside the crystals. The electric field of the optical excitation interacts with this macroscopic electric field in ways similar to the electrostrictive force of acoustic phonons[2] (Supporting Information). The force acted on the optical phonon will make work on the phonon oscillation. Depending on the positive or negative work acted on the phonon, the laser will enhance (heat) or attenuate (cool) the phonon oscillation.

The reverse of the energy flow direction in spontaneous Raman scattering

Crystalline ZnTe nanoribbon exhibits a zincblende structure belonging to the space group $T_d^2(F\bar{4}3M)$. Each unit cell of ZnTe contains two atoms. Consequently, there are 6 lattice dynamical modes: one degenerated transverse acoustic modes and one non-degenerated longitudinal acoustic modes, one degenerated transverse optical modes and one non-degenerated longitudinal optical modes[2,22]. The dispersion curves of all phonons along *L* symmetry direction

are schematically shown in Fig. 1a[22]. Due to the momentum conservation, only one specific LOP close to Brillouin zone center is involved in Raman scattering. In our case, this specific phonon is longitudinal optical phonon branch with $q \sim 2.0\times10^{-2}$ nm^{-1} ($q \sim 2\pi/\lambda_{laser}$, see Supporting Information part 1). Compared to the size of first Brillion zone $\pi/a \approx 5.0$ nm^{-1} ($a = 0.61$ nm is the lattice constant), we can conclude that the LOP involved in Raman scattering is the zone center phonon. Fig. 1b is the atomic displacement of LOP, a bulk vibration consisting of two counter-oscillating sub-lattices of Zn atoms and Te atoms. The LOP is a macroscopic excitation distributed over ~10^{16} atoms within the crystal and has a very high oscillating frequency owing to the strong interactions between neighboring atoms[2,23]. At the bath temperature of 225 K we conducted the experiments with a spectrometer broadening of ~39 GHz (see method and Fig. S1 in supporting information), the LOP's frequency is $\Omega_{LO}/2\pi = 6.23$ THz with a linewidth $\Gamma_{LO}/2\pi = 38$ GHz, corresponding a quality factor $Q_{LO} = 164$. The effective mass of LOP is $m_{\mathrm{LO}} = m_{Zn}m_{Te}/(m_{Zn}+m_{Te}) = 3.16\times10^{-28}\,\mathrm{kg}$ [2,22]. For the Fock states of LOP with well-defined quantized vibrational level $\bar{n}_{LO}$, the energy is $E = (\bar{n}_{LO}+1/2)\hbar\Omega_{LO}$, and the occupied probability of ground state $\bar{n}_{LO} = 0$ is $P_{\bar{n}_{LOP}=0} = 1/(1+\bar{n}_{LOP})$. The displacement of LOP is $\langle x^2 \rangle = k_B T/m_{LO}\Omega_{LO}^2$ [4-6,11]. At the quantum ground state $\bar{n}_{LO} = 0$, the zero-point fluctuation amplitude of LOP is $x_{zpf} = \sqrt{\hbar/2m_{LO}\Omega_{LO}} = 0.16$ nm[4,6,10,11]. Fig. 1c shows the Raman spectra of 120 nm ZnTe nanoribbon excited by a 0.1 mW 532 nm laser with the sample temperature varied from 340 to 77 K. As the temperature decreases, the exciton frequency gradually blue shifts. When the scattered photon frequency resonates with the exciton energy, *i.e.* $\omega_{ex} = \omega_{laser} \pm n\Omega_{LO}$ (n is an integer), the corresponding Raman peak of $n\Omega_{LO}$ shows the highest intensity. Therefore, the energy flow direction of Raman scattering can be reversed from phonon heating pumped at blue-resolved-sideband to phonon cooling at red-resolved-sideband pumping. As shown in Fig. 1c, the whole spectra are dominated by sharp Raman peaks with a weak broadband photoluminescence emission background. This dominance by Raman process is due to strong exciton-LOP coupling in our ZnTe nanobelt. Therefore, we can exclude the anti-Stokes fluorescence cooling process from the case of ZnTe nanobelts. Besides the electron-LOP coupling, the much narrower exciton peak in ZnTe compared to CdS[15] allows us to push the

sideband cooling into resolved regime, in which LOP Raman scattering is strongly enhanced. In the following paragraphs, we will discuss the resolved sideband Raman cooling and heating experiments in detail.

Experiments of Resolved sideband Raman cooling and heating of LO phonon

Figure 2a-d shows the basic principle and experimental setup of resolved-sideband cooling and heating, respectively. By tuning the detuned-frequency between laser and exciton, *i.e.* $\Delta = \omega_{laser} - \omega_{exciton}$, we can cool or heat the LOP. A pump-probe Raman thermometry[4,7] is used to detect the phonon occupation number $\overline{n}_{LO}$ and thus evaluate the effective temperature T_{LO} of phonons, where the phonon occupation follows the Bose-Einstein statistics $\overline{n}_{LO}(T) = \left(e^{\hbar\Omega_{LO}/k_B T} - 1\right)^{-1}$. In a cooling setup as shown in Fig. 2a, a red-detuned laser beam is used to pump the system, where the pump photons are scattered into the exciton resonance, thereby removing and cooling down the thermal vibration quanta of LOP from the ZnTe. Another blue-detuned laser beam with a power of 0.05 mW is used to probe the cooling behavior of LOP by monitoring its Stokes components. Based on the cooling theory[7,9-11,20] (see supporting information part 6 and 7), red-detuned driving laser will add extra damping Γ_{net} into the intrinsic LOP damping Γ_0 and decrease its occupation number (thus decrease the intensity of LOP) as shown in Fig. 2b. The experimental setup of LOP heating is reversed. A blue-detuned laser is used as a pump beam while the red-detuned laser is used as a probe beam. As shown in Fig. 2c, the blue-detuned laser scatters pump photons into the exciton cavity, thus creating phonons and leading to heating. This blue-detuned laser contributes an anti-damping into the LOP and leads to a LOP amplification, *i.e.* linewidth decreases and intensity increases. Here we choose resonant excitation $\Delta_{probe} \approx \pm\Omega_{LO}$ to enhance the probed Raman signal for cooling and heating experiments, respectively. Fig. 2e displays the experimental exciton emission spectra excited by 473 nm, Raman spectra excited by blue-detuned laser 532.19 nm, and by red-detuned laser 542.6 nm at the bath temperature of 225 K. At this temperature, exciton transition frequency is $\omega_{ex}(225\text{ K})/2\pi = 558.94$ THz, and its damping rate is $\kappa_{ex}(225\text{ K})/2\pi = 4.99$ THz, thus the quality factor $Q_{ex}(225\text{ K}) = 112$. The LOP's resolved-sideband resolution of exciton transition is $\Omega_{LO}/\kappa_{ex}(225\text{ K}) = 1.2$. For the cooling experiments, the 542.6 nm laser is the cooling laser and

532.19 nm laser is the probe laser, and *vice versa* for the heating experiments. In order to achieve the highest cooling efficiency, we let the exciton exactly resonates with the 1-LOP anti-Stokes photon scattered from red-detuned laser but slightly below the 1-LOP Stokes photon from blue-detuned laser, *i.e.* $\Delta_{anti-Stokes} = \omega_{anti-Stokes} - \omega_{exciton} = -\Omega_{LO}$ *and* $\Delta_{Stokes} = \omega_{Stokes} - \omega_{exciton} = 0.7\Omega_{LO}$. In heating experiments, we set the bath temperature to 230 K to meet $\Delta_{anti-Stokes} = \omega_{anti-Stokes} - \omega_{exciton} = -0.7\Omega_{LO}$ *and* $\Delta_{Stokes} = \omega_{Stokes} - \omega_{exciton} = \Omega_{LO}$. The laser heating effects can be excluded by analyzing the Raman peak change and monitoring the TOP (transverse optical phonon) and LOP of ZnTe as well as Raman peak of silicon substrate (see supporting information part 7.4).

The sequence of experiments is shown in Fig. 3a. First of all, we record the probed Stokes spectra of LOP without the pumping beam at a bath temperature of 225 K; then we record the probed Stokes spectra upon the laser beam pumping, where the acquired spectra are sum signal contributed from both the probe and pump beams. In order to subtract the background signal due to pump beam, we record the spectra due to pump beam alone by blocking the probe beam. Upon subtracting, we thus obtain the actual cooled LOP's spectra. Finally, we check the probe spectra by blocking the pump beam in order to exclude the sample drifting. Fig. 3b and Fig. 3c show the combined and subtracted spectra depending on the pumping power. As we increase the cooling laser power, the LOP peak becomes weaker and weaker. This is a result of resolved-sideband Raman cooling of LOP as we discussed above. Another interesting observation is that the LOP shows a composite lineshape profile of two Lorentzians as shown in Fig. 3d. There is a stronger and narrower LOP-like peak with a frequency $\omega^{-}/2\pi$ around 6.23 THz and a FWHM γ^{-} around 90 GHz, and another weaker and broader exciton-like peak $\omega^{+}/2\pi$ with a FWHM γ^{+} around 1.197 THz. With increasing of pump power, ω^{+} and ω^{-} became split more and more, and the intensity ratio of ω^{-} to ω^{+}decreases from 11 to 9.5. One of the possible explanations of this phenomena is the normal mode splitting induced by a strong coupling between the exciton and the LOP, which is similar as the phenomena that have been observed in trapped atoms[24], single quantum dots located in microcavity[25], and optomechanical system[10,12,26]. Different with optomechanical system, here the exciton-LOP coupling will form a new quasiparticle so called polaron as described by Fröhlich Hamiltonian[2,27] (see supporting information part 5). More experiments to explore the dispersion of these two coupling modes are necessary. Unfortunately

no suitable tunable laser source is available in the bandgap vicinity for the time being. By fitting these two modes, we can find that the red-detuned driving light field will dramatically change the frequency and linewidth of both LOP and exciton. In Fig. 3e, we plot the fitted frequency and damping rates of LOP depending on the cooling laser power. Consistent with the resolved-sideband cooling in optomechanical system [8-11], we also observed that the LOP is spring-softened ~ 7 GHz due to optical spring effect and experiences more damping rate ~ 15 GHz introduced by the red-detuned laser pumping. This extra damping of LOP demonstrates that the LOP experience a cooling process.

As discussed in supporting information (part 7), we use two thermometry methods to determine the LOP occupation number and effective temperature. The first one is based on the intensity ratio $\frac{\bar{n}_{LO}(P_{cl})+1}{\bar{n}_{LO}(P_{cl}=0)+1}=\frac{A_{Stokes}(\omega,P_{cl})}{A_{Stokes}(\omega,P_{cl}=0)}\frac{\left[[\Delta_{probe}(P_{cl})-\Omega_{LO}(P_{cl})]^2+\kappa_{ex}^2(P_{cl})\right]}{\left[[\Delta_{probe}(P_{cl}=0)-\Omega_{LO}(P_{cl}=0)]^2+\kappa_{ex}^2(P_{cl}=0)\right]}$, and the second one is the linewidth ratio $T_{final}=T_{initial}(\Gamma_{initial}/\Gamma_{final})$. As can been seen in Fig. 3d, it should be noted that the changes of frequency and linewidth of both exciton and LOP give rise to the resonant factor $\frac{\left[[\Delta_{probe}(P_{cl})-\Omega_{LO}(P_{cl})]^2+\kappa_{ex}^2(P_{cl})\right]}{\left[[\Delta_{probe}(P_{cl}=0)-\Omega_{LO}(P_{cl}=0)]^2+\kappa_{ex}^2(P_{cl}=0)\right]}$, which must be considered when we use intensity ratio equation. Usually，the amplitude of LOP Raman peak is prone to some system parameters such as drift. Although, we have used the check sequence to exclude such variations, nonetheless, an alternative thermometry should be established based on the damping of the LOP spectral linewidth, which is relatively immune to the amplitude disturbances.

We have shown the effective LOP occupation number and temperature in Fig. 3f based on the mentioned two thermometry methods: integrated intensity ratio and linewidth ratio. We conclude that the two thermometry methods unanimously show a consistent cooling value with a small discrepancy. Increasing the cooling pumping power from 0 to 1.1 mW, the occupation number of LOP decreases from 0.36 to 0.19, correspondingly the ground state occupation possibility increases from ~73.5% to 84.0% and effective temperature decreases from 225 K to 165 K. Increasing the pumping power further to more than 1.1 mW, the LOP occupation number and temperature is almost saturated at 0.19 and 165 K, respectively. It should be noted that

resolved sideband Raman cooling of LOP induced by extra driving light field experiences totally different damping process compared with the cooling effect of the whole sample. As shown in Fig. S2, when we cool the whole sample, *i.e.* decrease the bath temperature, the linewidth of LOP become narrower and narrower because the thermal fluctuation (anharmonicity effect) contribute less damping in lower temperature.

There are many interesting physical phenomena when the system is pumped at blue resolved-sideband, such as phonon lasing, squeezed state preparation and efficient entanglement between excitons and phonons [10,13,14,28,29]. As shown in Fig. 4, we have also demonstrated the heating of LO phonon pumped with a blue-detuned laser beam (532 nm). As shown in Fig. 4a, the experimental procedures are the same as the cooling experiments. We also use two methods to evaluate the heating effects as discussed in supporting information (part 7). As we increase the laser power from 0 mW to 0.19 mW, the occupation number increases and the effective temperature of the phonon modes also increases. As shown in Fig. 4b and Fig. 4c, in the heating process, the linewidth of LOP become narrower (Fig. 4c) and the intensity of LOP increases. However, as shown in Fig. 4d, the temperature and occupation of LOP calculated from two thermometry methods still show linear power dependence, suggesting that we did not observe stimulated optical amplification process or saying LOP lasing in our experiments. It is important if LOP lasing can be realized, because this LOP give a 6.23 THz frequency, which is very useful in THz applications. One possible solution is to make a cavity of this ZnTe nanostructure or put ZnTe gain materials into other optical cavity such as photonic crystals.

Another feature should be noted is that the linewidth of LOP shows a laser wavelength dependence even in the same bath temperature as shown in Fig. 4c, Fig. 3d, and Fig. S2. This is because phonon damping is very sensitive to the laser frequency due to optomechanical damping effect similar with cavity optomechanic system[10]: the extra damping introduced can be written as $\Gamma_{net} = g\left(\frac{\kappa_{ex}}{\kappa_{ex}^2/4+(\Delta+\Omega_{LOP})^2} - \frac{\kappa_{ex}}{\kappa_{ex}^2/4+(\Delta-\Omega_{LOP})^2}\right)$ and $\Gamma_{final} = \Gamma_0 + \Gamma_{net}$. By substituting the following parameters into the above equation: $\Delta = 0.7\Omega_{LOP}$ and $\Gamma_{final} = 38$ GHz for 532 nm excitation, $\Delta = -\Omega_{LOP}$ and $\Gamma_{final} = 102$ GHz for 543 nm excitation, we can get the coupling factor g =51 $(\text{GHz})^2$ and intrinsic linewidth $\Gamma_0 = 63$ GHz. It means that the optomechanical damping effect is the main reason of linewidth discrepancy with difference laser excitation.

Under off-resonance excitation of 514 nm, the measured linewidth of LOP ~70 GHz is close to its intrinsic linewidth ~63 GHz due to absence of coupling. However, the red-sideband excitation (543 nm) contributes positive damping due to strong red-sideband resonant pumping and thus lead to a broadened linewidth ~102 GHz. In the case of blue-sideband excitation (532 nm), it contributes negative heating anti-damping and thus has a narrower linewidth ~38 GHz.

Conclusion

In conclusion, by using the resolved-sideband excitation, we have demonstrated that the direction of the energy flow in Raman scattering can be tuned either upwards or downwards by detuning the pump laser with respect to the exciton transition involving a specific longitudinal optical phonon in semiconductor. Consequently, the cooling and heating of LOP are observed. Our work experimentally verifies the theoretical prediction of resolved-sideband Raman cooling of solid proposed more than 40 years ago[18,19] and confirms the speculation whether reversing energy flow is possible in Raman scattering in a recent experiment on Brillouin scattering cooling of acoustic phonon in optomechanics[20]. Our concept can also be extended to other solid-state system such as the coupling between LOP and single-electron spin in a diamond nitride vacancy (NV) center, in a similar manner of coupling between single-electron spin in a diamond NV center and magnetized atomic force microscopy (AFM) cantilever[30]. Furthermore, our results also supply a possible experimental solution to achieve net Raman cooling of solids as recently proposed by Rand[31] and Chen *et al.*[32]

Methods

The ZnTe nanoribbons were synthesized in a home-built, vapour-transport chemical-vapour-deposition system. The thickness of the nanobelts (100 nm in experiments) was measured by atomic force microscopy (Nanoscope III, Veeco Instruments). The details can be found in other references[27,33]. Three solid-state lasers of 473, 532 and 543 nm wavelengths were collimated and focused thorough a 50× objective onto the single ZnTe nanobelt that deposited on silicon substrates with a 100 nm oxide layer. All the spectra were collected using a confocal triple-grating spectrometer (Horiba-JY T64000) in a backscattering configuration. The 532 nm laser is single longitudinal mode with an intrinsic linewidth of 10 MHz but the 473 and 543 nm lasers are multi-longitudinal modes. The spectrometer resolution of 39 GHz is determined by measuring the linewidth of a 532 nm laser, which is approximately equal to spectrometer resolution considering very narrow intrinsic linewidth of 532 nm laser. In this paper, the spectrometer broadening of 39 GHz has been subtracted from all of linewidth data. The measured linewidth of multi-mode 543 laser is 169 GHz as shown in Fig. S1. The single frequency laser around 543 nm is obtained by purifying the multi-modes 543 laser with 1800 g/mm Horiba HR320 monochromator with a 100 micrometer slit and a size tunable pinhole at the T64000 spectrometer. The distance is around 3 meters from the output slit of HR320 to the pinhole. By controlling the wavelength position, slit width and pinhole size, we can obtain 8 single frequency output around 543 nm with spectrum linewidth of 45 GHz. In our measurements, we choose the strongest mode at 552.25 THz as the excitation laser. The error bars only consider the fitting error. For ZnTe, the exciton transition energy tends to increase with a decreasing bath temperature. Here we control the bath temperature to tune the exciton transition energy in order to match our laser wavelengths of 532.19 nm (563.32 THz) and 542.58 nm (552.25 THz).

Acknowledgments: The authors acknowledge Professors Myungshik S Kim for the stimulating discussions. J.Z. acknowledges the support from the National Natural Science Foundation of China (Grant No. 11574305 and 51527901), and the National Young 1000 Talent Plan of China. Z. J and Q. X. acknowledge the support by LU JIAXI International team program supported by K.C. Wong Education Foundation and CAS. Q.X. acknowledges the strong support from the Singapore National Research Foundation through a Fellowship grant (NRF-RF2009-06) and an Inestigatorship Award (NRF-NRFI2015-03), and Singapore Ministry of Education via two Tier 2 grants (MOE2011-T2-2-051 and MOE2013-T2-1-049). Q.X. also gratefully acknowledges the partial support from Asian Office of Aerospace Research and Development (AOARD, FA2386-13-1-4112), an international office under the United State Air Force Office of Scientific Research (AFOSR).

Author contributions

J.Z. and Q.X. conceived the idea. J.Z. designed the experiments. J.Z., Q.Z. and X.W. performed the experiments and prepared the samples. J.Z., L.K. and Q.X. analyzed the data and wrote the manuscript. All authors read and commented the manuscript.

Additional Information

The authors declare no competing financial interests. Supplementary information is given at the website www.nature.com/naturephotonics. All correspondence and request of materials should be addressed to J.Z or Q.X.

References:

1 Robert W., B. *Nonlinear Optics*. 2 edn, p394 (Academic Press, 2003).

2 Yu, P. Y. & Cardona, M. *Fundamentals of Semiconductors: Physics and Materials Properties*. 3 edn, p375 (Springer, 2005).

3 Chu, S. Nobel Lecture: the manipulation of neutral particles. *Rev. Mod. Phys.* **70**, 685-706, (1998).

4 Diedrich, F., Bergquist, J. C., Itano, W. M. & Wineland, D. J. Laser cooling to the zero-point energy of motion. *Phys. Rev. Lett.* **62**, 403-406, (1989).

5 Leibfried, D., Blatt, R., Monroe, C. & Wineland, D. Quantum dynamics of single trapped ions. *Rev. Mod. Phys.* **75**, 281-324, (2003).

6 Wieman, C. E., Pritchard, D. E. & Wineland, D. J. Atom cooling, trapping, and quantum manipulation. *Rev. Mod. Phys.* **71**, S253-S262, (1999).

7 Wineland, D. J., Itano, W. M., Bergquist, J. C. & Hulet, R. G. Laser-cooling limits and single-ion spectroscopy. *Phys. Rev. A* **36**, 2220-2232, (1987).

8 Chan, J. *et al.* Laser cooling of a nanomechanical oscillator into its quantum ground state. *Nature* **478**, 89-92, (2011).

9 Kippenberg, T. J. & Vahala, K. J. Cavity optomechanics: back-action at the mesoscale. *Science* **321**, 1172-1176, (2008).

10 Markus, A., Tobias J., K. & Florian, M. Cavity optomechanics. *Rev. Mod. Phys.* **86**, 1391-1452, (2014).

11 Teufel, J. D. *et al.* Sideband cooling of micromechanical motion to the quantum ground state. *Nature* **475**, 359-363, (2011).

12 Verhagen, E. *et al.* Quantum-coherent coupling of a mechanical oscillator to an optical cavity mode. *Nature* **482**, 63-67, (2012).

13 Clerk, A. A. *et al.* Introduction to quantum noise, measurement, and amplification. *Rev. Mod. Phys.* **82**, 1155-1208, (2010).

14 Spillane, S. M., Kippenberg, T. J. & Vahala, K. J. Ultralow-threshold Raman laser using a spherical dielectric microcavity. *Nature* **415**, 621-623, (2002).

15 Zhang, J., Li, D., Chen, R. & Xiong, Q. Laser cooling of a semiconductor by 40 Kelvin. *Nature* **493**, 504-508, (2013).

16 Epstein, R. I. *et al.* Observation of laser-induced fluorescent cooling of solid. *Nature* **377**, 500-503, (1995).

17 Ha, S.-T., Shen, C., Zhang, J. & Xiong, Q. Laser cooling of organic–inorganic lead halide perovskites. *Nature Photon.* **10**, 115-121, (2016).

18 Dykman, M. I. Relaxation of impurities in a nonresonant field and phonon amplification. *Sov. J. Low Temp. Phys.* **5**, 89-95, (1979).

19 Dykman, M. I. Heating and cooling of local and quasilocal vibration by a nonresonance field. *Sov. Phys. Solid State* **20,**, 1306-1311, (1978).

20 Bahl, G., Tomes, M., Marquardt, F. & Carmon, T. Observation of spontaneous Brillouin cooling. *Nature Phys.* **8**, 203-207, (2012).

21 Grudinin, I. S., Lee, H., Painter, O. & Vahala, K. J. Phonon Laser Action in a Tunable Two-Level System. *Phys. Rev. Lett.* **104**, 083901, (2010).

22 Madelung, O., Rössler, U. & Schulz, M. *Landolt-Bornstein Numerical Data and Functional Relationships in Science and Technology, Group III: Condensed Matter. Semiconductors: II-VI and I-VII compounds, Vol. 41B.* p159 (Springer, 1999).

23 Lee, K. C. *et al.* Entangling macroscopic diamonds at room temperature. *Science* **334**, 1253-1256, (2011).
24 Haroche, S. & Kleppner, D. Cavity quantum electrodynamics. *Phys. Today* **42**, 24-30, (1989).
25 Khitrova, G. *et al.* Vacuum Rabi splitting in semiconductors. *Nature Phys.* **2**, 81-90, (2006).
26 Groblacher, S., Hammerer, K., Vanner, M. R. & Aspelmeyer, M. Observation of strong coupling between a micromechanical resonator and an optical cavity field. *Nature* **460**, 724-727, (2009).
27 Zhang, Q. *et al.* Highly Enhanced Exciton Recombination Rate by Strong Electron–Phonon Coupling in Single ZnTe Nanobelt. *Nano Lett.* **12**, 6420-6427, (2012).
28 Vahala, K. *et al.* A phonon laser. *Nature Phys.* **5**, 682-686, (2009).
29 Bahl, G., Zehnpfennig, J., Tomes, M. & Carmon, T. Stimulated optomechanical excitation of surface acoustic waves in a microdevice. *Nature Commun.* **2**, 403, (2011).
30 Kolkowitz, S. *et al.* Coherent sensing of a mechanical resonator with a single-spin qubit. *Science* **335**, 1603-1606, (2012).
31 Rand, S. C. Raman laser cooling of solids. *J. Lumines.* **133**, 10-14, (2013).
32 Chen, Y.-C. & Bahl, G. Raman cooling of solids through photonic density of states engineering. *Optica* **2**, 893-899, (2015).
33 Utama, M. I. B. *et al.* The Growth of Ultralong ZnTe Micro/Nanostructures: The Influence of Polarity and Twin Direction on the Morphogenesis of Nanobelts and Nanosheets. *Cryst. Growth Des.* **13**, 2590-2596, (2013).

Resolved Sideband Raman Cooling of an Optical Phonon in Semiconductor Materials

Jun Zhang[1,2,], Qing Zhang[1], Xingzhi Wang[1], Leong Chuan Kwek[3,4], and Qihua Xiong[1,5,6,]**

[1]Division of Physics and Applied Physics, School of Physical and Mathematical Sciences, Nanyang Technological University, 637371, Singapore.

[2]State Key Laboratory of Superlattices and Microstructures, Institute of Semiconductors, Chinese Academy of Sciences, Beijing, 100083, China

[3]Centre for Quantum Technologies, National University of Singapore, 3 Science Drive 2, 117543, Singapore

[4]National Institute of Education and Institute of Advanced Studies, Nanyang Technological University, 1 Nanyang Walk, 637616, Singapore

[5]NOVITAS, Nanoelectronics Center of Excellence, School of Electrical and Electronic Engineering, Nanyang Technological University, 639798, Singapore.

[6]MajuLab, CNRS-UNS-NUS-NTU International Joint Research Unit, UMI 3654, Singapore

*Correspondence should be addressed to Email:zhangjwill@semi.ac.cn, Qihua@ntu.edu.sg

Figures and Captions

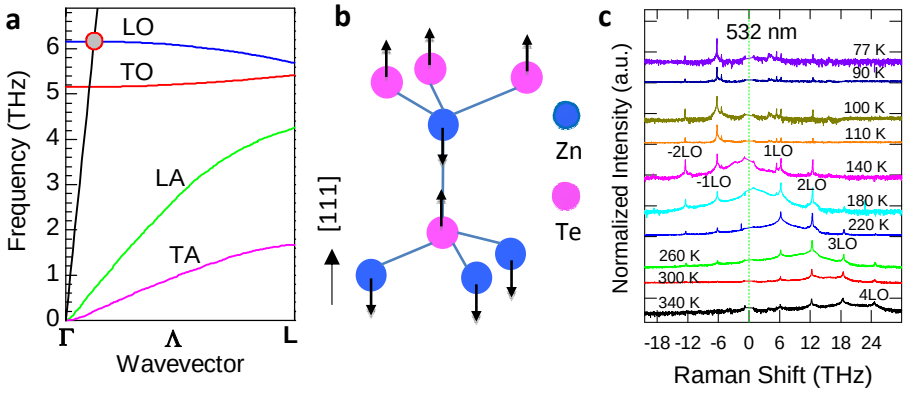

Figure 1. Crystalline structure and LOP modes of zincblende semiconductor ZnTe. **a**, The phonon dispersion curves of ZnTe. The color curves are the phonons of ZnTe and the black line is the dispersion of light. The red circle corresponds the detectable phonon frequency in the experiments. **b**, The vibrational normal mode of the LOP. **c**, Raman spectra of ZnTe nanoribbons at various temperatures. The intensity is displayed in logarithmic scale with base 10. The sharp peaks are the multi-order LOP modes. When the scattered light resonates with the exciton emission, the corresponding phonon peak shows the highest enhancements. Negative Raman shift corresponds to anti-Stokes process.

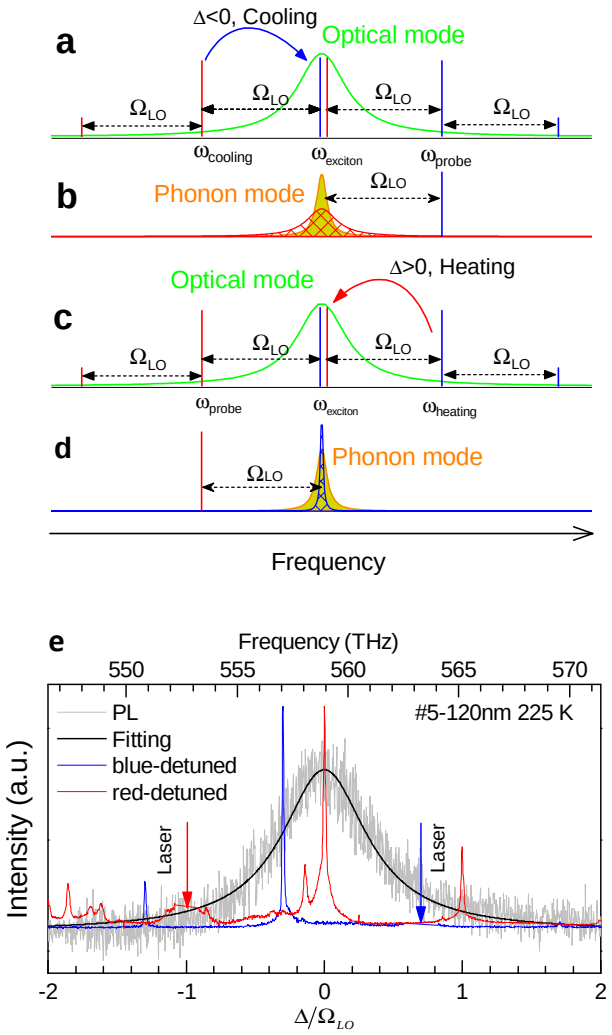

Figure 2. Principle of the resolved-sideband cooling and amplification in semiconductors. **a**, Pump-probe Raman thermometry for resolved-sideband cooling experiments. The red-detuned cooling laser (detuned energy $\Delta=\omega_{cooling}-\omega_{exciton}<0$) resided to the LOP anti-Stokes resolved-sideband of exciton transition favors to scattering the photons upwards to the exciton transition by annihilating the LOPs, thus it reverses the energy flow direction and leads to cooling of LOPs. A weak probe beam resided at the blue-detuned resolved-sideband is used to detect the phonon occupation number by monitoring its Stokes spectrum of LOP. **b**, With increasing of cooling laser power, the LOP's occupation number reduces and its damping rate increases. For the amplification processes, the blue-detuned laser is used as a heating beam and red-detuned laser is probe beam as shown in **c** and **d**. **e**, The measured experimental spectra of exciton transition, Stokes spectra of LOP with blue-detuned laser and anti-Stokes spectra of LOP with red-detuned laser. The bath temperature is settled at 225 K.

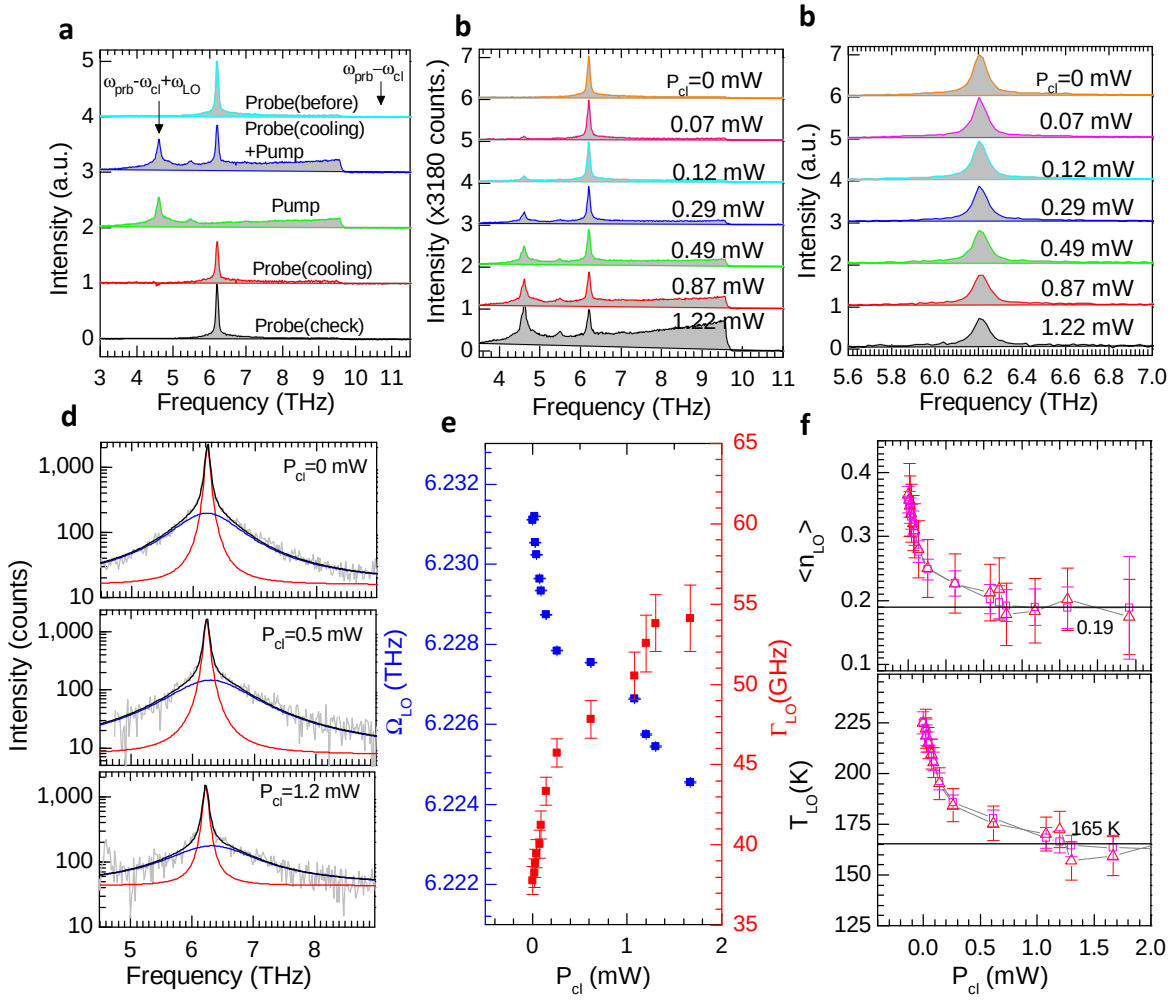

Figure 3. Resolved-sideband cooling results of LOP pumped at red-detuned resolved-sideband. **a,** Measurement sequences. ω_{prb} and ω_{cl} represent the probing and cooling laser frequency, respectively. **b**, The combined spectra depending on the power of cooling laser. **c**, Probed Stokes spectra of LOP after subtracting the background signal deduced from the cooling laser beam. **d**, Double Lorentzian fitting of LOP's Stokes spectra selected from the **c**, with three different laser powers. **e**, Power dependence of frequency and damping rates of LOP. **f**, Occupation number and the temperature of LOP versus the power of cooling laser. Two thermometry methods were used here: integrated intensity ratio (red open triangles), linewidth ratio (pink open squares).

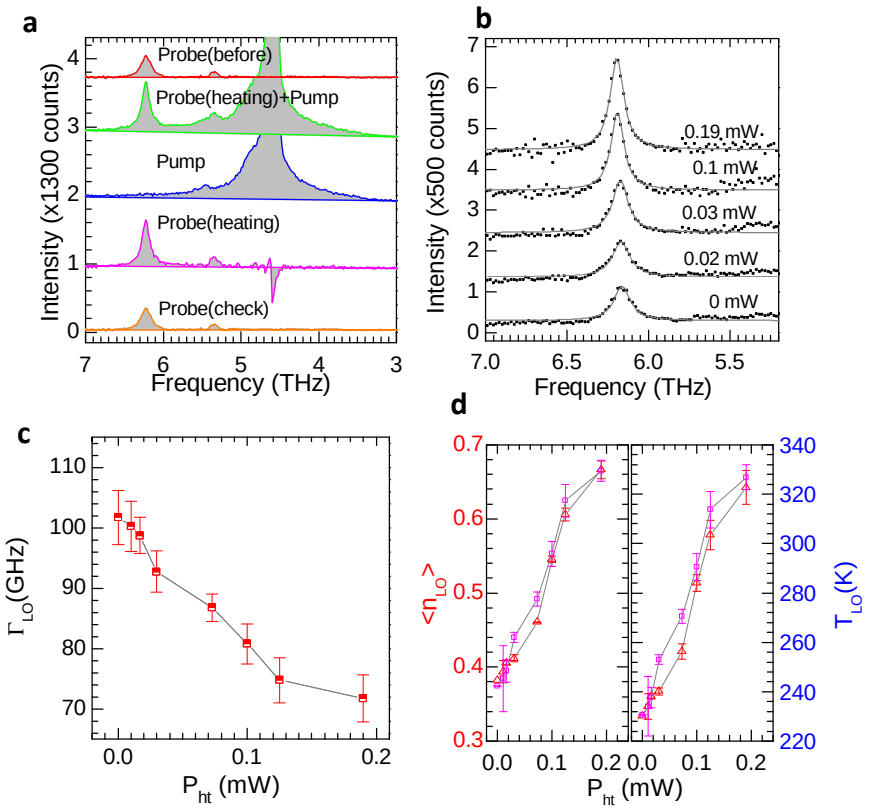

Figure 4. Amplification results of LOP pumped at blue-detuned resolved-sideband. a, The spectra of sequential measurements. The intense peak at ~ 4.6 THz is the anti-Stokes LOP Raman peak due to pump beam (532 nm). **b**, The anti-Stokes spectra probed by the red-detuned laser depend on the heating laser power at blue-detuned resolved-sideband. **c**, The damping rates of LOP depending on the heating laser power. The multi-modes laser induced broadening has already been subtracted. **d**, The occupation number and effective temperatures of LOP depending on the power of heating laser. Two thermometry methods were used here: integrated intensity ratio (red open triangles) and linewidth ratio (pink open squares).